Robust determination of optical path difference: fringe tracking at the Infrared Optical Telescope Array interferometer

Ettore Pedretti, Wesley A. Traub, John D. Monnier, Rafael Millan-Gabet, Nathaniel P. Carleton, F. Peter Schloerb, Michael K. Brewer, Jean-Philippe Berger, Marc G. Lacasse, and Sam Ragland

We describe the fringe-packet tracking system used to equalize the optical path lengths at the Infrared Optical Telescope Array interferometer. The measurement of closure phases requires obtaining fringes on three baselines simultaneously. This is accomplished by use of an algorithm based on double Fourier interferometry for obtaining the wavelength-dependent phase of the fringes and a group-delay tracking algorithm for determining the position of the fringe packet. A comparison of data acquired with and without the fringe-packet tracker shows a factor of ~3 reduction of the error in the closure-phase measurement. The fringe-packet tracker has been able so far to track fringes with signal-to-noise ratios as low as 1.8 for stars as faint as $m_H = 7.0$.

OCIS codes: 120.0120, 120.2650, 120.3180.

1. Introduction

Observations performed with long-baseline ground-based optical–infrared interferometers are strongly affected by the turbulent atmosphere. Turbulence can reduce the visibility of fringes in many ways, as described by Porro *et al.*[1] for pupil-plane (or coaxial) beam combinations and Thureau[2] for image-plane beam combinations. Turbulence randomly modulates the phases of the fringes, which can then become unusable for image reconstruction. Using three or more telescopes removes the atmospheric phase contamination. This is done through the closure-phase technique pioneered in radio astronomy[3] and only recently applied to long-baseline optical interferometry.[4] The necessary condition for obtaining meaningful closure phases is that the three fringe packets be detected within the coherence time, which one achieves by keeping the optical path difference (OPD) to a minimum.

Before 2002, the Infrared Optical Telescope Array (IOTA) interferometer had only two telescopes and a single baseline, and the fringes were usually kept inside the scan interval manually by the observers. The installation of a third telescope at the IOTA interferometer required an increase in the level of automation in the instrument because manual tracking is not practical with three baselines to adjust. In particular, the requirement to measure closure phases necessitated a system that is capable of keeping the fringe packets in the center of the scan by use of the existing hardware dedicated to acquiring data. Fringes must be acquired in the same coherence time if one is to measure a closure phase. This is especially important at the IOTA interferometer, where the bandwidths are frequently relatively large (15%–25%) and the fringe packets quite narrow (three to six fringes).

We present here a simple and fast algorithm, that uses double Fourier interferometry[5] to extract wavelength-dependent information from the fringe packet and calculate its group delay. The same algorithm was independently discovered by Tubbs[6] and written in a final-year undergraduate project that was never published. In that report Tubbs tested the algorithm through simulated data and data obtained

E. Pedretti (epedrett@umich.edu), W. A. Traub, N. P. Carleton, M. G. Lacasse, and S. Ragland are with the Smithsonian Astrophysical Observatory, 60 Garden Street, Cambridge, Massachusetts 02138. J. Monnier and E. Pedretti are with the University of Michigan, Ann Arbor, Michigan 48109. R. Millan-Gabet is with the Michelson Science Center, California Institute of Technology, Pasadena, California 91125. F. P. Schloerb and M. K. Brewer are with the University of Massachusetts, Amherst, Massachusetts 01003. J.-P. Berger is with the Laboratoire d'Astrophysique de Grenoble, B.P. 53 X, Grenoble Cedex 9, France.

Received 9 November 2004; revised manuscript received 29 March 2005; accepted 31 March 2005.

0003-6935/05/255173-07$15.00/0

from the Cambridge Optical Aperture Synthesis Telescope (COAST) interferometer but did not implement a working fringe-packet tracker. We became aware of that research only after our algorithm was routinely used at the IOTA interferometer.

The time-domain interferograms recorded by an infrared detector for the purpose of measuring the physical parameters of stellar objects are used to track the positions of fringes. A fringe packet is generated by pupil-plane interference of starlight from two telescopes, where the OPD about the zero-path-difference point is changed linearly with time. Each pair of three telescopes generates two such interferograms, with complementary intensities. The goal is to control the optical paths such that these interferograms occur nearly simultaneously, such that the closure phase can be measured from them. To do this, we apply the algorithm in the present paper to each fringe packet, and the output of the algorithm is used to control the optical paths before the next interferogram is produced. As many as ~10 interferograms are generated per second, by triangular sweeps of the optical paths. No additional hardware is required.

The application of the algorithm is not restricted to stellar interferometry but can be applied to all cases when broadband interference fringes must be tracked. Other algorithms for fringe-packet tracking that have been tested at the IOTA interferometer are the subjects of separate publications.[7–11]

2. The Instrument

The IOTA is a long-baseline optical interferometer located at the Smithsonian Institution's Whipple Observatory on Mount Hopkins, Arizona, and comprises three 45 cm diameter telescopes that can be positioned at 17 stations on an L-shaped track, where the arms are 15 m toward the southeast and 35 m toward the northeast. The IOTA interferometer operated with two telescopes from 1995 to 2003 and has had three telescopes since February 2002. The interferometer[12,13] has been used as a testbed for new cutting-edge technologies[14–16] and has produced astronomy results in the three-telescope configuration.[17–21]

The three beams arriving from the vacuum delay-line tank hit three dichroic mirrors, which separate visible and infrared light. The visible beam continues toward the star tracker servo system. In the implementation discussed here, the infrared beam is reflected toward three flat mirrors and then three off-axis parabolas, which focus the three beams on three single-mode (*H* band) fibers feeding the IONIC-3T integrated-optics beam combiner.[22]

Interference is achieved inside the integrated-optics component, resulting in three output pairs that are π radi out of phase in intensity. The interference fringes are recorded while two of the dichroics are piezo driven to scan paths of approximately $+50$ μm and -50 μm, respectively, to scan through the fringe packet in the three beams. The six combined beams are then focused onto six separate pixels of the PICNIC array[16] and recorded as time series for science measurement. The same time series is used by the fringe-packet tracker. The path difference calculated by the packet tracker is fed back to the piezo scanning dichroics for a fast tracking response. The piezo scanners are off-loaded of their additional offsets every second, when a fraction of the error signal is sent to the short delay lines that are responsible for tracking the geometric delay caused by the rotation of the Earth.

3. Calculating the Fringe Position

A. Tracking the Fringe Packet by Double Fourier Interferometry

Our method of fringe-packet tracking at the IOTA interferometer calculates the group delay of fringes dispersed with double Fourier interferometry, which we use to obtain the wavelength-dependent phase from the fringe packet. We do this by scanning the fringe packet over an interval greater than the packet length, where the spectral resolution is proportional to the scan length. The group-delay tracking method has been applied to interferometry since the very beginning of the discipline, when Michelson[23] used a prism for dispersing and acquiring fringes visually at the 20 ft. (6.096 m) interferometer. Labeyrie[24] used the same system and demonstrated fringe acquisition on a two-telescope interferometer.

Several systems have been proposed for correcting the optical path since then.[25,26] Group-delay tracking (also called dispersed fringe tracking when it is applied to image plane interferometry) has been routinely used at several interferometric facilities.[27–29] In fact, at the IOTA interferometer's group-delay tracking was selected as the original method of path difference monitoring in the visible,[30–33] but the system was set aside in favor of making infrared observations.

We now perform a derivation of the algorithm for a two-telescope interferometer that combines the light in the pupil plane through a beam splitter. With this setup the intensity of light $I(\xi)$ from the two complementary outputs of the beam splitter is measured by square-law detectors:

$$I(\xi) = I_t\left\{1 \pm V\,\frac{\sin[\pi(\xi-\xi_0)\Delta f]}{\pi(\xi-\xi_0)\Delta f}\,\sin[2\pi(\xi-\xi_0)f_0+\phi]\right\}, \tag{1}$$

where I_t is the mean intensity, which is split by the beam combiner ($\pm$ represent complementary outputs) and is modulated by the interferometric signal, a function of optical path ξ. V is the contrast of the fringes, $\Delta f\,[\mathrm{cm}^{-1}]$ is the bandwidth of the ideal (rectangular) spectral filter, $f_0\,[\mathrm{cm}^{-1}]$ is the frequency of the fringe, ϕ [rad] is a generic phase, and ξ_0 [cm] is the fringe-packet center, which varies from scan to scan owing to atmospheric-path fluctuation. This is the actual value that we want to calculate to correct the optical path.

In practice we are dealing with discrete intensities,

expressed as a finite series of data, so we can rewrite Eq. (1) as the discrete function $n(j)$, which is the detector count:

$$n(j) = n_0\left\{1 \pm V\,\frac{\sin[\pi(j - J_0)\Delta m]}{\pi(j - J_0)\Delta m}\,\sin[2\pi(j - J_0)m_0 + \phi]\right\} + \epsilon_j. \tag{2}$$

Here n_0 is the mean number of electrons per channel and V is the fringe visibility. Sample number j ranges from 1 to N, where N is the total number of samples; typically $N = 256$. The center of the fringe packet is at sample J_0. If the high- and low-wave-number limits of the spectral filter are written as m_h and m_l (waves per sample), then the filter's full width at half-maximum is $\Delta m = m_h - m_l$, and the filter's center is $m_0 = (m_h + m_l)/2$, both in units of waves (or fringes) per sample. Phase ϕ [rad] is an offset between the sinusoid carrier wave and the center of the sinc envelope. The ϵ_j term represents additive noise, the sum of electron counting statistics, detector read noise, and random atmospheric scintillation. The goal is to extract an estimate of J_0 from the ensemble of N data points.

The first step is to calculate the fast Fourier transform of the data string $n(j)$ and scale the result to eliminate uninteresting factors. The result is a sequence of $N/2$ complex numbers that can be written as

$$\tilde{n}(m_0) = \exp(-i2\pi m_0 J_0) + \eta_{m_0}, \tag{3}$$

where η_{m_0} is the scaled transform of noise term ϵ_j.

The second step is to select two of the $\tilde{n}$ values, say, $\tilde{n}(m_0)$ and $\tilde{n}(m_0 + \Delta m_{12})$, and form the cross-spectrum product of the first with the complex conjugate of the second, i.e.,

$$X(m_0,\ m_0 + \Delta m_{12}) = \tilde{n}(m_0)\tilde{n}(m_0 + \Delta m_{12})^*. \tag{4}$$

As can be seen from Eq. (3), cross spectrum X will generate a complex number (plus noise) whose phase contains the unknown quantity J_0, multiplied by known terms. The additive noise would degrade our estimate of J_0 from the cross-spectrum term; however, adding several such terms will improve the signal-to-noise ratio (SNR) of the resultant complex term[34] and likewise improve our estimate of J_0.

The third step is to calculate the average cross spectrum $\bar{X}$, for example, in

$$\bar{X} = \sum_{m_0=m_l}^{m_h} \frac{X(m_0,\ m_0 + \Delta m_{12})}{(m_h - m_l + 1)} = \exp(-i2\pi\Delta_{m12}J_0) + \bar{\eta}, \tag{5}$$

where $\bar{\eta}$ is the new noise term, presumably smaller than the root mean square of η_{m_0} by a factor of the order of $(m_h - m_{l+1})^{1/2}$. The limits on the sum are only suggested values and could be changed to improve the signal-to-noise ratio, if applicable. (We note that the cross-spectrum is also used in the Knox–Thompson algorithm[35] for recovering near-diffraction-limited images of stellar objects from snapshots degraded by atmospheric seeing.)

The estimated fringe-packet position $\langle J_0\rangle$ can now be recovered from the average cross spectrum:

$$\langle J_0\rangle = \frac{\arg(\bar{X})}{2\pi\Delta m_{12}}. \tag{6}$$

Here the estimated packet center $\langle J_0\rangle$ is measured in units of sample numbers from the first point in the interferogram. In practice we subtract $N/2$ from this value and send the resultant value (suitably scaled) as an error signal to the servo system, such that the starting point of the next scan is adjusted accordingly.

We note that any value of Δm_{12} could be used, but we suggest that $\Delta m_{12} = 1$ is optimum in the sense that it is least likely to produce a complex S or $\bar{S}$ that is biased by wrap-around effects, which will occur if the phase shifts between adjacent values of $\tilde{n}$ are separated by more than π. Hereafter we drop the expectation value brackets and write J_0 instead of $\langle J_0\rangle$ for notational simplicity.

B. Algorithm Summary

1. The interference fringes are recorded while two of the optical paths are piezo driven to scan paths of approximately $+50$ and -50 μm. Time series n_j is recorded by the infrared camera for the three pairs of beams.
2. Fast Fourier transform $\tilde{n}(m_0)$ of time series n_j is computed separately for the three pairs.
3. We calculate cross spectrum X for the three beams by multiplying $\tilde{n}(n_0)$ by its complex conjugate $\tilde{n}^*(m_0 + 1)$ shifted by one sample.
4. Average cross spectrum $\bar{X}$ is computed relative to the fringe peak in the cross-power-spectrum to average the complex vector with a higher signal-to-noise ratio.
5. The position of the fringe packets is obtained from the phase of average vector $\bar{X}$ by use of Eq. (6).

C. Baseline Bootstrapping

With baseline bootstrapping[36,37] we are able to blind track fringes on a baseline when the SNR of the fringes is too low, provided that good SNRs are available on the other two baselines. For this reason we calculate optical path J_0 for three baselines, even if we correct the path for two baselines. We can express one optical path as the weighted average of the other two optical paths, where the weights are equal to the SNR for the fringes obtained on those baselines. We calculate the SNR from cross spectrum $|X|^2$, dividing the averaged power inside the fringe peak by the averaged power outside the fringe peak. We then observe that the optical path in a closed loop must be

equal to zero:

$$J_0 1 + J_0 2 + J_0 3 = 0 \tag{7}$$

where $J_0 1$ and $J_0 2$ are the optical paths where the servo loop is acting, while $J_0 3$ is the reference optical path. To paths $J_0 1$, $J_0 2$, and $J_0 3$ are associated weights $w1$, $w2$, and $w3$, respectively. We have two values for each optical path. One is the value obtained directly on that baseline (for example, $J_0 1$ with weight $w1$); the other is the value calculated from the linear combination of the other two baselines [for example, $J_0 1' = -J_0 2 - J_0 3$ with weight $w1' = (w2w3)/(w2 + w3)$]. The weighted average of J_0 and J'_0 can then be written as[38]

$$\overline{J_0 1} = \frac{w1 J_0 1 + w1' J_0 1'}{w1 + w1'}, \tag{8}$$

where $\overline{J_0 1}$ is the weighted-averaged path difference. Similarly for $\overline{J_0 2}$:

$$\overline{J_0 2} = \frac{w2 J_0 2 + w2' J_0 2'}{w2 + w2'},$$

$$J_0 2' = -J_0 1 - J_0 3,$$

$$w2' = \frac{w1 w3}{w1 + w3}. \tag{9}$$

The advantage of using a weighting system is that we do not have to select the best baseline values *a priori* but rather that the weighting allows them to be selected automatically.

4. Simulations

The linearity of the fringe-packet tracker (FPT) algorithm was tested through simulations. This simulation was performed in presence of photon and detector noise, with an average number of 300 photoelectrons/sample for the fringe intensity (Poisson distributed), a fringe visibility of 1, and an additional 12-electron mean of Gaussian noise for the detector.

It was found that the algorithm is capable of detecting the sign of the correction that is necessary to bring back the fringes to the center of the scan, even if the main part of the fringe packet is outside the current scan. The necessary condition is to have a sufficient SNR that the sidelobes are detectable. This behavior is shown in Fig. 1.

The returned position depends linearly on the fringe positions when the packet is inside the scan, but it is nonlinear when the packet is outside the scan. Nevertheless the information of the sidelobes can still be used to bring the fringes back to the center of the scan. The algorithm is sensitive to the slope of the phase across the bandwidth, and the sign of the correction is preserved. The algorithm starts to fail at the limit of the range where the signal is too low and the sidelobes are not detectable for the given integration time. The returned position depends linearly on the fringe positions when the packet is inside the scan and becomes strongly nonlinear (but with the correct sign) when the packet is outside the scan.

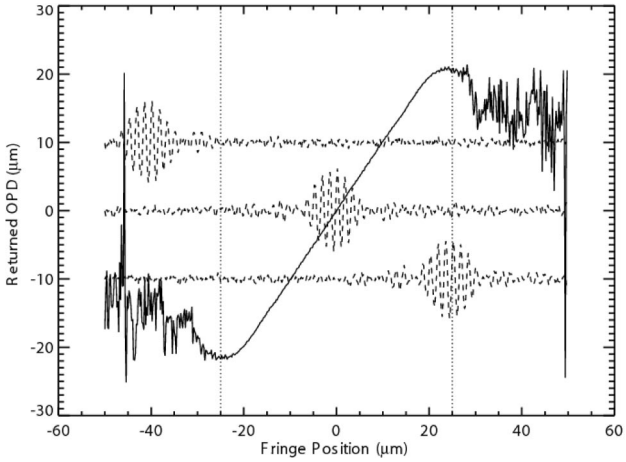

Fig. 1. Optical path returned by the algorithm versus fringe position (solid curve). The two vertical dotted curves represent the interval inside of which the fringes are sampled, for a scan length of 50 μm. Three fringe packets (dashed curves) mark three representative positions on the plot: outside the scan range (top), at the center of the scan (center), and half outside the scan range (bottom). Note that only the sidelobes are visible in the scan range of the plot at the top.

5. Results

The FPT has been in routine use at the IOTA interferometer since early 2002. Figure 2 shows the reduction of tracking residuals operated by the algorithm. A reduction of a factor of ~2 in the rms change of the optical path, between data acquired with tracking switched off compared with data with tracking on, can be shown from the recorded data. This reduction

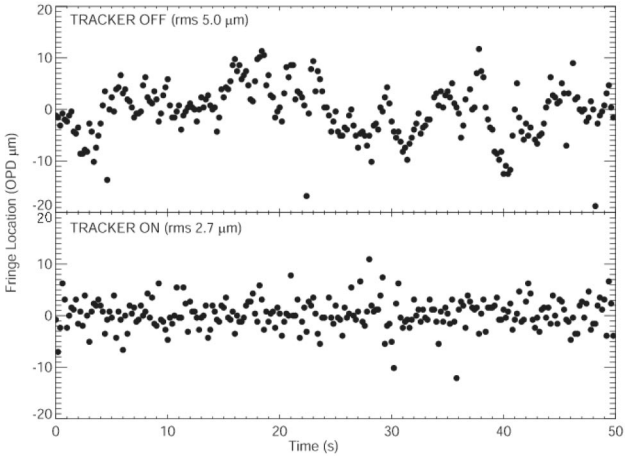

Fig. 2. Change in OPD with the FPT turned off (top) and turned on (bottom). This experiment was performed with a single, 21 m long baseline at 1.65 μm during average seeing and no baseline bootstrapping. The data were recorded on 6 March 2002. We measured a factor-of-2 reduction in the rms change in optical path.

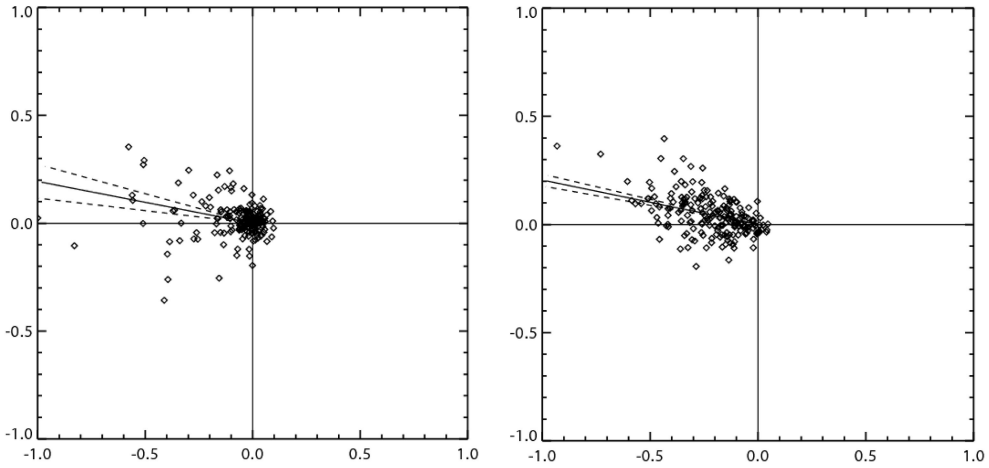

Fig. 3. Closure phase measurement for the star WR140 ($m_H = 5.3$). The points represented on the plot are complex vectors normalized by the SNR. Each point was calculated by use of a single fringe measurement for each baseline (notably the N–S, N–W, and W–S baselines, where the telescopes were positioned at $N = 35$ m, $S = 15$ m, and $W = 10$ m). There are 200 points for each diagram. The vector represented by solid lines is the average closure phase of the previous 200 vectors, and the dashed lines represent the error on the closure phase. Finally, a closure-phase measurement in open-loop mode (FPT not active; closure phase, 169.0° ± 4.3°) is shown at the left, whereas the closed-loop mode (FPT active; closure phase, 168.4° ± 1.5° deg) is shown at the right.

lies mostly in the low-frequency zone because of the limited bandwidth of the combined fringe sensor–fringe actuator. For the IOTA interferometer this is a significant improvement, as the high-frequency phase noise is dealt within postprocessing by use of the closure-phase information.

It is in fact more important to be able to maintain the superposition of the fringe packet and to be able to do so for faint sources rather than to reduce the residuals of the OPD to a smaller value. Figure 3 shows two measurements of closure phase. When the FPT is switched off, the closure phase is 169.0° ± 4.3°, but it is 168.4° ± 1.5° when the FPT is operating (a factor-of-3 error reduction for the closed-loop case).

We also show that the FPT is capable of tracking fringes on a 7.0 m_H star with a SNR as low as 1.8, as shown in Fig. 4.

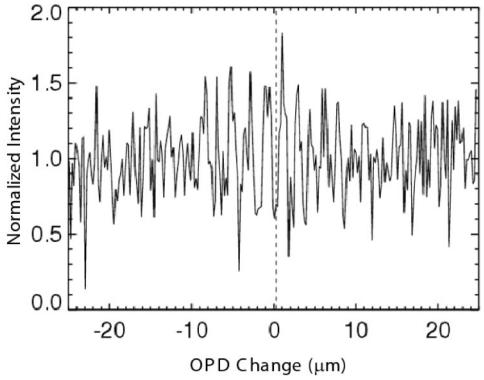

Fig. 4. Faint fringe observed on a 7.0 m_H star, yielding a SNR of 1.8. The dashed line shows the expected position calculated by the FTP.

6. Conclusions

We have described the fringe-packet tracking system now routinely in use at the IOTA interferometer. The packet tracker uses existing hardware to perform its functions, notably the infrared camera used for data acquisition, as a fringe sensor and the fringe-scanning platforms, combined with the delay lines, for correcting the optical path. It is based on an algorithm that exploits the wavelength-dependent information contained in the fringe packet, which is extracted by use of double Fourier interferometry. The phase of the fringes obtained for different frequencies is used for calculating the group delay of the fringe packet. As we use baseline bootstrapping, we are capable of blind tracking fringes on a baseline when their SNR is low, provided that the fringes have a good SNR on the other two baselines of the interferometer.

We used numerical simulation to model a fringe packet outside the scanning range operated by the algorithm when only the sidelobes of the fringe packet are visible. We also have shown that the fringe-packet tracker algorithm effectively reduces the slowly varying atmospheric and instrumentally induced additional path, leaving the fast phase noise to be dealt with postprocessing. Moreover, the FPT delivers a factor-of-~3 reduction of the error in the closure-phase measurement and has been able so far to track fringes with SNRs as low as 1.8.

This research was made possible by a Smithsonian predoctoral fellowship and a Michelson postdoctoral fellowship awarded to E. Pedretti. The IONIC project is a collaboration among the Laboratoire d'Astrophysique de Grenoble, the Laboratoire d'Electromagnetisme Microondes et Optoelectronique, and also the Commissariat a l'Energie

Atomique–Laboratoire d'Electronique de Technologie et d'Instrumentation and the Institut de Microélectronique, Électromagnétisme et Photonique, Grenoble, France. The IONIC project is funded in France by the Centre National de Recherche Scientifique and the Centre National d'Etudes Spatiales. The research and the operation of the fringe-packet tracker were supported in part by grant NAG5-4900 from NASA, by grants AST-0138303 from the National Science Foundation, and by funds from the Smithsonian Institution. This research has made use of NASA's Astrophysics Data System bibliographic services.

References

1. I. L. Porro, W. A. Traub, and N. P. Carleton, "Effect of telescope alignment on a stellar interferometer," Appl. Opt. **38,** 6055–6067 (1999).
2. N. D. Thureau, "Contribution à l'interférométrie optique à longue base en mode multi-tavelures," Ph.D. dissertation (Université de Nice-Sophia Antipolis, 2001).
3. R. C. Jennison, "A phase sensitive interferometer technique for the measurement of the Fourier transforms of spatial brightness distributions of small angular extent," Mon. Not. R. Astron. Soc. **118,** 276–284 (1958).
4. J. E. Baldwin, M. G. Beckett, R. C. Boysen, D. Burns, D. F. Buscher, G. C. Cox, C. A. Haniff, C. D. Mackay, N. S. Nightingale, J. Rogers, P. A. G. Scheuer, T. R. Scott, P. G. Tuthill, P. J. Warner, D. M. A. Wilson, and R. W. Wilson, "The first images from an optical aperture synthesis array: mapping of Capella with COAST at two epochs," Astron. Astrophys. **306,** L13–L16 (1996).
5. J.-M. Mariotti and S. T. Ridgway, "Double Fourier spatio-spectral interferometry—combining high spectral and high spatial resolution in the near infrared," Astron. Astrophys. **195,** 350–363 (1988).
6. R. N. Tubbs, "Tracking and characterising atmospheric phase fluctuations at COAST," Part III; undergraduate project rep. Cavendish Laboratory, Cambridge University (1998); http://www.geocities.com/CapeCanaveral/2309/phase_track.html.
7. E. Wilson and R. W. Mah, "Online fringe tracking and prediction at IOTA," in *18th Congress of the International Commission for Optics*, A. J. Glass, J. W. Goodman, M. Chang, A. H. Guenther, and T. Asakura, eds., Proc. SPIE **3749,** 691–692 (1999).
8. S. Morel, W. A. Traub, J. D. Bregman, R. W. Mah, and E. Wilson, "Fringe-tracking experiments at the IOTA interferometer," in *Interferometry in Optical Astronomy*, P. J. Lena and A. Quirrenbach, eds., Proc. SPIE **4006,** 506–513 (2000).
9. N. D. Thureau, R. C. Boysen, D. F. Buscher, C. A. Haniff, E. Pedretti, P. J. Warner, and J. S. Young, "Fringe envelope tracking at COAST," in *Interferometry for Optical Astronomy II*, W. A. Traub, ed., Proc. SPIE **4838,** 956–963 (2003).
10. E. Wilson, E. Pedretti, J. D. Bregman, R. Mah, and W. A. Traub, "Adaptive DFT-based interferometer fringe tracking," EURASIP J. Appl. Signal Process. (to be published).
11. E. Wilson, E. Pedretti, J. D. Bregman, R. Mah, and W. A. Traub, "Adaptive DFT-based fringe tracking and prediction at IOTA," in *New Frontiers in Stellar Interferometry*, W. A. Traub, ed., Proc. SPIE **5491,** 1108–1112 (2004).
12. W. A. Traub, N. P. Carleton, J. D. Bregman, M. K. Brewer, M. G. Lacasse, P. Maymounkov, R. Millan-Gabet, J. D. Monnier, S. Morel, C. D. Papaliolios, M. R. Pearlman, I. L. Porro, F. P. Schloerb, and K. Souccar, "Third telescope project at the IOTA interferometer," in *Interferometry in Optical Astronomy*, P. J. Lena and A. Quirrenbach, eds., Proc. SPIE **4006,** 715–722 (2000).
13. W. A. Traub, A. Ahearn, N. P. Carleton, J. Berger, M. K. Brewer, K. Hofmann, P. Y. Kern, M. G. Lacasse, F. Malbet, R. Millan-Gabet, J. D. Monnier, K. Ohnaka, E. Pedretti, S. Ragland, F. P. Schloerb, K. Souccar, and G. Weigelt, "New beam-combination techniques at IOTA," in *Interferometry for Optical Astronomy II*, W. A. Traub, ed., Proc. SPIE **4838,** 45–52 (2003).
14. J. P. Berger, P. Haguenauer, P. Kern, K. Perraut, F. Malbet, I. Schanen, M. Severi, R. Millan-Gabet, and W. Traub, "Integrated optics for astronomical interferometry. IV. First measurements of stars," Astron. Astrophys. **376,** L31–L34 (2001).
15. J. D. Monnier, J. P. Berger, R. Millan-Gabet, W. A. Traub, N. P. Carleton, E. Pedretti, C. M. Coldwell, and C. D. Papaliolios, "SMART precision interferometry at 794 nm," in *Interferometry for Optical Astronomy*, W. A. Traub, ed., Proc. SPIE **4838,** 1127–1138 (2003).
16. E. Pedretti, R. Millan-Gabet, J. D. Monnier, W. A. Traub, N. P. Carleton, J.-P. Berger, M. G. Lacasse, F. P. Schloerb, and M. K. Brewer, "The PICNIC interferometry camera at IOTA," Publ. Astron. Soc. Pac. **116,** 377–389 (2004).
17. J. D. Monnier, R. Millan-Gabet, P. G. Tuthill, W. A. Traub, N. P. Carleton, V. Coude du Foresto, W. C. Danchi, M. G. Lacasse, S. Morel, G. Perrin, and I. Porro, "Aperture synthesis using multiple facilities: Keck aperture masking and the IOTA interferometer," in *Interferometry for Optical Astronomy*, W. A. Traub, ed., **4838,** 379–386 (2003).
18. K. Ohnaka, U. Beckman, J. P. Berger, M. K. Brewer, K. Hofmann, M. G. Lacasse, V. Malanushenko, R. Millan-Gabet, E. Pedretti, J. D. Monnier, D. Schertl, F. P. Schloerb, V. Shenavrin, and W. A. Traub, "IOTA observation of the circumstellar envelope of R CrB," in *Interferometry for Optical Astronomy*, W. A. Traub, ed., **4838,** 1068–1071 (2003).
19. R. Millan-Gabet, E. Pedretti, J. D. Monnier, W. A. Traub, F. P. Schloerb, N. P. Carleton, S. Ragland, M. G. Lacasse, W. C. Danchi, P. Tuthill, G. Perrin, and V. Coudé du Foresto, "Recent science results from the two-telescope IOTA," in *Interferometry for Optical Astronomy*, W. A. Traub, ed., Proc. SPIE **4838,** 202–209 (2003).
20. G. Weigelt, U. Beckman, J. P. Berger, T. Bloecker, M. K. Brewer, K. Hofmann, M. G. Lacasse, V. Malanushenko, R. Millan-Gabet, J. D. Monnier, K. Ohnaka, E. Pedretti, D. Schertl, F. P. Schloerb, M. Scholz, W. A. Traub, and B. Yudin, "JHK-band spectro-photometry of T Cep with the IOTA interferometer," in *Interferometry for Optical Astronomy*, W. A. Traub, ed. Proc. SPIE **4838,** 181–184 (2003).
21. J. D. Monnier, W. A. Traub, F. P. Schloerb, R. Millan-Gabet, J.-P. Berger, E. Pedretti, N. P. Carleton, S. Kraus, M. G. Lacasse, M. Brewer, S. Ragland, A. Ahearn, C. Coldwell, P. Haguenauer, P. Kern, P. Labeye, L. Lagny, F. Malbet, D. Malin, P. Maymounkov, S. Morel, C. Papaliolios, K. Perraut, M. Pearlman, I. L. Porro, I. Schanen, K. Souccar, G. Torres, and G. Wallace, "First results with the IOTA3 imaging interferometer: the spectroscopic binaries λ Virginis and WR 140," Astrophys. J. **602,** L57–L60 (2004).
22. J. Berger, P. Haguenauer, P. Y. Kern, K. Rousselet-Perraut, F. Malbet, S. Gluck, L. Lagny, I. Schanen-Duport, E. Laurent, A. Delboulbe, E. Tatulli, W. A. Traub, N. Carleton, R. Millan-Gabet, J. D. Monnier, E. Pedretti, and S. Ragland, "An integrated-optics 3-way beam combiner for IOTA," in *Interferometry for Optical Astronomy II*, W. A. Traub, ed., Proc. SPIE **4838,** 1099–1106 (2003).
23. A. A. Michelson and F. G. Pease, "Measurement of the diameter of alpha Orionis with the interferometer," Astrophys. J. **53,** 249–259 (1921).
24. A. Labeyrie, "Interference fringes obtained on Vega with two optical telescopes," Astrophys. J. **196,** L71–L75 (1975).
25. F. Vakili and L. Koechlin, "Aperture synthesis in space—

computer fringe blocking," in *New Technologies for Astronomy*, J.-P. Swings, ed., Proc. SPIE **1130,** 109–116 (1989).
26. Y. Rabbia, S. Menardi, J. Gay, P. M. Bourlon, P. Antonelli, M. Dugue, J. Marchal, F. Reynaud, M. Faucherre, and N. Hubin, "Prototype for the European Southern Observatory VLTI fringe sensor," in *Amplitude and Intensity Spatial Interferometry II*, J. B. Breckinridge, ed., Proc. SPIE **2200,** 204–215 (1994).
27. S. Robbe, B. Sorrente, F. Cassaing, Y. Rabbia, G. Rousset, L. Dame, P. Cruzalebes, and G. Schumacher, "Active phase stabilization at the I2T: implementation of the ASSI table," in *Amplitude and Intensity Spatial Interferometry II*, J. B. Breckinridge, ed., Proc. SPIE **2200,** 222–230 (1994).
28. P. R. Lawson, "Group-delay tracking in optical stellar interferometry with the fast Fourier transform," J. Opt. Soc. Am. A **12,** 366–374 (1995).
29. L. Koechlin, P. R. Lawson, D. Mourard, A. Blazit, D. Bonneau, F. Morand, P. Stee, I. Tallon-Bosc, and F. Vakili, "Dispersed fringe tracking with the multi-r_0 apertures of the Grand Interferometre a 2 Telescopes," Appl. Opt. **35,** 3002–3009 (1996).
30. P. Nisenson and W. Traub, "Magnitude limit of the group delay fringe tracking method for long baseline interferometry," in *Interferometric Imaging in Astronomy*, J. W. Goad, ed., (European Space Observatory, 1987), pp. 129–134.
31. W. A. Traub and M. G. Lacasse, "Laboratory measurements of visibility using dispersed fringes in wavenumber space," in *NOAO-ESO Conference on High-Resolution Imaging by Interferometry: Ground-Based Interferometry at Visible and Infrared Wavelengths*, F. Merkle, ed., Vol. 29 of ESO Conference and Workshop Proceedings (European Southern Observatory, 1988), pp. 947–954.
32. W. A. Traub, "Constant-dispersion grism spectrometer for channeled spectra," J. Opt. Soc. Am. A **7,** 1779–1791 (1990).
33. W. A. Traub, M. G. Lacasse, and N. P. Carleton, "Spectral dispersion and fringe detection in IOTA," in *Amplitude and Intensity Spatial Interferometry*, J. B. Breckinridge, ed., Proc. SPIE 145–152 (1990).
34. D. F. Buscher, "Getting the most out of C.O.A.S.T.," Ph.D. dissertation (University of Cambridge, 1988).
35. K. T. Knox and B. J. Thompson, "Recovery of images from atmospherically degraded short-exposure photographs," Astrophys. J. **193,** L45–L48 (1974).
36. F. Roddier, in "High-resolution imaging by interferometry," in *NOAO-ESO Conference on High-Resolution Imaging by Interferometry: Ground-Based Interferometry at Visible and Infrared Wavelengths*, F. Merkle, ed., Vol. 29 of ESO Conference and Workshop Proceedings (European Southern Observatory, 1988), pp. 565–571.
37. J. T. Armstrong, D. Mozurkewich, L. J. Rickard, D. J. Hutter, J. A. Benson, P. F. Bowers, N. M. Elias, C. A. Hummel, K. J. Johnston, D. F. Buscher, J. H. Clark, L. Ha, L.-C. Ling, N. M. White, and R. S. Simon, "The Navy prototype optical interferometer," Astrophys. J. **496,** 550–571 (1998).
38. P. R. Bevington and D. K. Robinson, *Data Reduction and Error Analysis for the Physical Sciences*, 2nd ed. (McGraw-Hill, 1992).